MIRROR CURVE OF ORBIFOLD HURWITZ NUMBERS

OLIVIA DUMITRESCU and MOTOHICO MULASE

Communicated by Mirela Babalic

Edge-contraction operations form an effective tool in various graph enumeration problems, such as counting Grothendieck's dessins d'enfants and simple and double Hurwitz numbers. These counting problems can be solved by a mechanism known as topological recursion, which is a mirror B-model corresponding to these counting problems. We show that for the case of orbifold Hurwitz numbers, the mirror objects, i.e., the spectral curve and the differential forms on it, are constructed solely from the edge-contraction operations of the counting problem in genus 0 and one *marked* point. This forms a parallelism with Gromov-Witten theory, where genus 0 Gromov-Witten invariants correspond to mirror B-model holomorphic geometry.

AMS 2010 Subject Classification: Primary 14N35, 81T45, 14N10; Secondary 53D37, 05A15.

Key words: topological recursion, ribbon graphs, Hurwitz numbers, mirror curves.

1. INTRODUCTION

The purpose of the present paper is to identify the mirror B-model objects that enable us to solve certain graph enumeration problems. We consider simple and orbifold Hurwitz numbers, by giving a graph enumeration formulation for these numbers. We then show that the mirror of these counting problems are constructed from the *edge-contraction operations* of [8] applied to orbifold Hurwitz numbers for the case of *genus* 0 *and one-marked point*.

Edge-contraction operations provide an effective method for graph enumeration problems. It has been noted in [11] that the Laplace transform of edge-contraction operations on many counting problems corresponds to the topological recursion of [14]. In this paper, we examine the construction of mirror B-models corresponding to the simple and orbifold Hurwitz numbers. In general, enumerative geometry problems, such as computation of Gromov-Witten type invariants, are often solved by studying a corresponding problem on the *mirror dual* side. The effectiveness of the mirror method relies on complex analysis and holomorphic geometry technique that is available on the mirror B-model side. The question we consider in this paper is the following:

The first author is supported by NSF grant DMS1802082.

Question 1.1. How do we find the mirror of a given enumerative problem?

We give an answer to this question for a class of graph enumeration problems that are equivalent to counting orbifold Hurwitz numbers. The key is the edge-contraction operations. The base case, or the case for the "moduli space" $\overline{\mathcal{M}}_{0,1}$, of the edge contraction in the counting problem identifies the mirror dual object, and a universal mechanism of complex analysis, known as the **topological recursion** of [14], solves the B-model side of the counting problem. The solution is a collection of generating functions of the original counting problem for all genera.

Bouchard and Mariño [3] conjectured that generating functions for simple Hurwitz numbers could be calculated by the topological recursion of [14], based on the spectral curve identified as the **Lambert curve**

$$x = ye^{-y}. \tag{1.1}$$

Here, the notion of spectral curve is the mirror dual object for the counting problem. They arrived at the mirror dual by a consideration of mirror symmetry of *open* Gromov-Witten invariants of toric Calabi-Yau threefolds [2]. The mirror geometry of a toric Calabi-Yau threefold is completely determined by a plane algebraic curve known as the *mirror curve*. The Lambert curve (1.1) appears as the infinite framing number limit of the mirror curve of $\mathbb{C}^3$. The Hurwitz number conjecture of [3] was then solved in a series of papers by one of the authors [13, 21], using the Lambert curve as a *given* input. Since conjecture is true, the Lambert curve (1.1) *should be* the mirror B-model for Hurwitz numbers. But why? In [13, 21], we did not attempt to give any explanation.

The emphasis of our current paper is to prove that the mirror dual object is simply a consequence of the $\overline{\mathcal{M}}_{0,1}$ case of the edge-contraction operation on the original counting problem. The situation is similar to several cases of Gromov-Witten theory, where the mirror is constructed by the genus 0 Gromov-Witten invariants themselves.

To illustrate the idea, let us consider the number T_d of connected *trees* consisting of *labeled* d nodes (or vertices). The initial condition is $T_1 = 1$. The numbers satisfy a recursion relation

$$(d-1)T_d = \frac{1}{2}\sum_{\substack{a+b=d\\ a,b\geq 1}} ab\binom{d}{a}T_aT_b. \tag{1.2}$$

A tree of d nodes has $d-1$ edges. The left-hand side counts how many ways we can eliminate an edge. When an edge is eliminated, the tree breaks down into two disjoint pieces, one consisting of a labeled nodes, and the other $b = d - a$ labeled nodes. The original tree is restored by connecting one of the a nodes on

one side to one of the b nodes on the other side. The equivalence of counting in this elimination process gives (1.2). From the initial value, the recursion formula generates the tree sequence $1, 1, 3, 16, 125, 1296, \ldots$. We note, however, that (1.2) does not directly give a closed formula for T_d. To find one, we introduce a generating function, or a **spectral curve**

$$y = y(x) := \sum_{d=1}^{\infty} \frac{T_d}{(d-1)!} x^d. \tag{1.3}$$

In terms of the generating function, (1.2) becomes equivalent to

$$\left(x^2 \circ \frac{\mathrm{d}}{\mathrm{d}x} \circ \frac{1}{x}\right) y = \frac{1}{2} x \frac{\mathrm{d}}{\mathrm{d}x} y^2 \Longleftrightarrow \frac{\mathrm{d}x}{\mathrm{d}y} = \frac{x(1-y)}{y}. \tag{1.4}$$

The initial condition is $y(0) = 0$ and $y'(0) = 1$, which allows us to solve the differential equation uniquely. Lo and behold, the solution is exactly (1.1).

To find the formula for T_d, we need the *Lagrange Inversion Formula*. Suppose that $f(y)$ is a holomorphic function defined near $y = 0$, and that $f(0) \neq 0$. Then the inverse function of $x = \frac{y}{f(y)}$ near $x = 0$ is given by

$$y = \sum_{k=1}^{\infty} \left(\frac{\mathrm{d}}{\mathrm{d}y}\right)^{k-1} \left(f(y)^k\right)\Big|_{y=0} \frac{x^k}{k!}. \tag{1.5}$$

The proof is elementary and requires only Cauchy's integration formula. Since $f(y) = e^y$ in our case, we immediately obtain Cayley's formula $T_d = d^{d-2}$.

The point we wish to make here is that the real problem behind the scene is not tree-counting, but *simple Hurwitz numbers*. This relation is understood by the correspondence between trees and ramified coverings of $\mathbb{P}^1$ by $\mathbb{P}^1$ of degree d that are simply ramified except for one total ramification point. When we look at the dual graph of a tree, elimination of an edge becomes contracting an edge, and this operation precisely gives a *degeneration formula* for counting problems on $\overline{\mathcal{M}}_{g,n}$. The base case for the counting problem is $(g, n) = (0, 1)$, and the recursion (1.2) is the result of the edge-contraction operation for simple Hurwitz numbers associated with $\overline{\mathcal{M}}_{0,1}$. In this sense, the Lambert curve (1.1) is the *mirror dual* of simple Hurwitz numbers.

The paper is organized as follows. In Section 2, we present combinatorial graph enumeration problems, and show that they are equivalent to counting of simple and orbifold Hurwitz numbers. In Section 3, the spectral curves of the topological recursion for simple and orbifold Hurwitz numbers (the mirror objects to the counting problems) are constructed from the edge-contraction formulas for $(g, n) = (0, 1)$ invariants.

2. ORBIFOLD HURWITZ NUMBERS AS GRAPH ENUMERATION

Mirror symmetry provides an effective tool for counting problems of Gromov-Witten type invariants. The question is how we construct the mirror, given a counting problem. Although there is so far no general formalism, we present a systematic procedure for computing orbifold Hurwitz numbers in this paper. The key observation is that the edge-contraction operations for $(g, n) = (0, 1)$ identify the mirror object.

The topological recursion for simple and orbifold Hurwitz numbers are derived as the Laplace transform of the cut-and-join equation [1, 13, 21], where the spectral curves are identified by the consideration of mirror symmetry of toric Calabi-Yau orbifolds [1, 3, 15, 16]. In this section we give a purely combinatorial graph enumeration problem that is equivalent to counting orbifold Hurwitz numbers. We then show in the next section that the edge-contraction formula restricted to the $(g, n) = (0, 1)$ case determines the spectral curve and the differential forms $W_{0,1}$ and $W_{0,2}$ of [1]. These quantities form the mirror objects for the orbifold Hurwitz numbers.

2.1. Cell graphs

To avoid unnecessary confusion, we use the terminology *cell graphs* in this article, instead of more common ribbon graphs. Ribbon graphs naturally appear for encoding complex structures of a topological surface (see for example, [18, 19]). Our purpose of using ribbon graphs are for degeneration of stable curves, and we label vertices, instead of *faces*, of a ribbon graph.

Definition 2.1 (Cell graphs). A connected **cell graph** of topological type (g, n) is the 1-skeleton of a cell-decomposition of a connected closed oriented surface of genus g with n labeled 0-cells. We call a 0-cell a *vertex*, a 1-cell an *edge*, and a 2-cell a *face*, of the cell graph. We denote by $\Gamma_{g,n}$ the set of connected cell graphs of type (g, n). Each edge consists of two **half-edges** connected at the midpoint of the edge.

Remark 2.2.

• The *dual* of a cell graph is a ribbon graph, or Grothendieck's dessin d'enfant. We note that we label vertices of a cell graph, which corresponds to face labeling of a ribbon graph. Ribbon graphs are also called by different names, such as embedded graphs and maps.

• We identify two cell graphs if there is a homeomorphism of the surfaces that brings one cell-decomposition to the other, keeping the labeling of 0-cells.

The only possible automorphisms of a cell graph come from cyclic rotations of half-edges at each vertex.

Definition 2.3 (Directed cell graph). A **directed cell graph** is a cell graph for which an arrow is assigned to each edge. An arrow is the same as an ordering of the two half-edges forming an edge. The set of directed cell graphs of type (g, n) is denoted by $\vec{\Gamma}_{g,n}$.

Remark 2.4. A directed cell graph is a *quiver*. Since our graph is drawn on an oriented surface, a directed cell graph carries more information than its underlying quiver structure. The tail vertex of an arrowed edge is called the *source*, and the head of the arrow the *target*, in the quiver language.

An effective tool in graph enumeration is edge-contraction operations. Often edge contraction leads to an inductive formula for counting problems of graphs.

Definition 2.5 (Edge-contraction operations). There are two types of **edge-contraction operations** applied to cell graphs.

• **ECO 1**. Suppose there is a directed edge $\vec{E} = \overrightarrow{p_i p_j}$ in a cell graph $\gamma \in \vec{\Gamma}_{g,n}$, connecting the tail vertex p_i and the head vertex p_j. We *contract* $\vec{E}$ in γ, and put the two vertices p_i and p_j together. We use i for the label of this new vertex, and call it again p_i. Then we have a new cell graph $\gamma' \in \vec{\Gamma}_{g,n-1}$ with one less vertices. In this process, the topology of the surface on which γ is drawn does not change. Thus genus g of the graph stays the same.

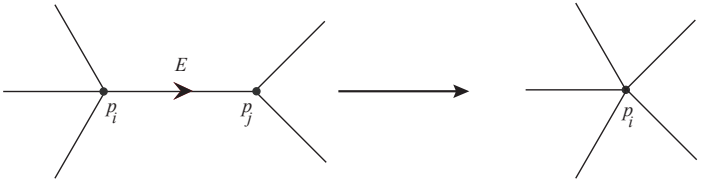

Figure 2.1 – Edge-contraction operation ECO 1. The edge bounded by two vertices p_i and p_j is contracted to a single vertex p_i.

• We use the notation $\vec{E}$ for the edge-contraction operation

$$\vec{E} : \vec{\Gamma}_{g,n} \ni \gamma \longmapsto \gamma' \in \vec{\Gamma}_{g,n-1}. \tag{2.1}$$

• **ECO 2**. Suppose there is a directed loop $\vec{L}$ in $\gamma \in \vec{\Gamma}_{g,n}$ at the i-th vertex p_i. Since a loop in the 1-skeleton of a cell decomposition is a topological cycle on the surface, its contraction inevitably changes the topology of the

surface. First we look at the half-edges incident to vertex p_i. Locally around p_i on the surface, the directed loop $\vec{L}$ separates the neighborhood of p_i into two pieces. Accordingly, we put the incident half-edges into two groups. We then break the vertex p_i into two vertices, p_{i_1} and p_{i_2}, so that one group of half-edges are incident to p_{i_1}, and the other group to p_{i_2}. The order of two vertices is determined by placing the loop $\vec{L}$ *upward* near at vertex p_i. Then we name the new vertex on its left by p_{i_1}, and on its right by p_{i_2}.

Let γ' denote the possibly disconnected graph obtained by contracting $\vec{L}$ and separating the vertex to two distinct vertices labeled by i_1 and i_2.

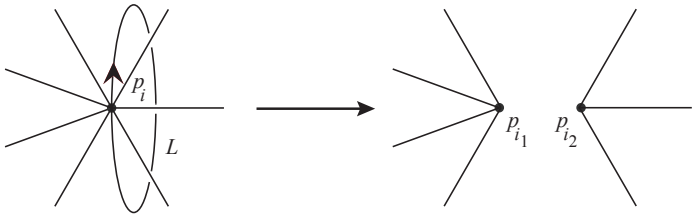

Figure 2.2 – Edge-contraction operation ECO 2. The contracted edge is a loop $\vec{L}$ of a cell graph. Place the loop so that it is upward near at p_i to which $\vec{L}$ is attached. The vertex p_i is then broken into two vertices, p_{i_1} on the left, and p_{i_2} on the right. Half-edges incident to p_i are separated into two groups, belonging to two sides of the loop near p_i.

• If γ' is connected, then it is in $\vec{\Gamma}_{g-1,n+1}$. The loop $\vec{L}$ is a *loop of handle*. We use the same notation $\vec{L}$ to indicate the edge-contraction operation

$$\vec{L} : \vec{\Gamma}_{g,n} \ni \gamma \longmapsto \gamma' \in \vec{\Gamma}_{g-1,n+1}. \tag{2.2}$$

• If γ' is disconnected, then write $\gamma' = (\gamma_1, \gamma_2) \in \vec{\Gamma}_{g_1,|I|+1} \times \vec{\Gamma}_{g_2,|J|+1}$, where

$$\begin{cases} g = g_1 + g_2 \\ I \sqcup J = \{1, \dots, \widehat{i}, \dots, n\} \end{cases} . \tag{2.3}$$

The edge-contraction operation is again denoted by

$$\vec{L} : \vec{\Gamma}_{g,n} \ni \gamma \longmapsto (\gamma_1, \gamma_2) \in \vec{\Gamma}_{g_1,|I|+1} \times \vec{\Gamma}_{g_2,|J|+1}. \tag{2.4}$$

In this case we call $\vec{L}$ a *separating loop*. Here, vertices labeled by I belong to the connected component of genus g_1, and those labeled by J are on the other component of genus g_2. Let (I_-, i, I_+) (reps. (J_-, i, J_+)) be the reordering of $I \sqcup \{i\}$ (resp. $J \sqcup \{i\}$) in the increasing order. Although we give labeling i_1, i_2 to the two vertices created by breaking p_i, since they belong to distinct graphs,

we can simply use i for the label of $p_{i_1} \in \gamma_1$ and the same i for $p_{i_2} \in \gamma_2$. The arrow of $\vec{L}$ translates into the information of ordering among the two vertices p_{i_1} and p_{i_2}.

Remark 2.6. The use of directed cell graphs enables us to define edge-contraction operations, keeping track with vertex labeling. We refer to [10] for the actual motivation for quiver cell graphs. Since our main concern is enumeration of graphs, the extra data of directed edges does not plan any role. In what follows, we deal with cell graphs without directed edges. The edge-contraction operations are defined with a choice of direction, but the counting formula we derive does not depend of this choice.

Remark 2.7. Let us define $m(\gamma) = 2g - 2 + n$ for a graph $\gamma \in \Gamma_{g,n}$. Then every edge-contraction operation reduces $m(\gamma)$ exactly by 1. Indeed, for ECO 1, we have

$$m(\gamma') = 2g - 2 + (n-1) = m(\gamma) - 1.$$

The ECO 2 applied to a loop of handle produces

$$m(\gamma') = 2(g-1) - 2 + (n+1) = m(\gamma) - 1.$$

For a separating loop, we have

$$\begin{array}{rc} & 2g_1 - 2 + |I| + 1 \\ +) & 2g_2 - 2 + |J| + 1 \\ \hline & 2g_1 + 2g_2 - 4 + |I| + |J| + 2 \end{array} \quad = \quad 2g - 2 + n - 1.$$

2.2. r-Hurwitz graphs

We choose and fix a positive integer r. The decorated graphs we wish to enumerate are the following.

Definition 2.8 (r-Hurwitz graph). An r-**Hurwitz graph** (γ, D) of type (g, n, d) consists of the following data.

- γ is a connected cell graph of type (g, n), with n labeled vertices.

- $|D| = d$ is divisible by r, and γ has $m = d/r$ unlabeled faces and s unlabeled edges, where

$$s = 2g - 2 + \frac{d}{r} + n. \tag{2.5}$$

- D is a configuration of $d = rm$ unlabeled dots on the graph subject to the following conditions:

1. The set of d dots are grouped into m subsets of r dots, each of which is equipped with a cyclic order.

2. Every face of γ has cyclically ordered r dots.

3. These dots are clustered near vertices of the face. At each corner of the face, say at Vertex i, the dots are ordered according to the cyclic order that is consistent of the orientation of the face, which is chosen to be counter-clock wise.

4. Let μ_i denote the total number of dots clustered at Vertex i. Then $\mu_i > 0$ for every $i = 1, \dots, n$. Thus we have an ordered partition

$$d = \mu_1 + \cdots + \mu_n. \tag{2.6}$$

In particular, the number of vertices ranges $0 < n \leq d$.

5. Suppose an edge E connecting two distinct vertices, say Vertex i and j, bounds the same face twice. Let p be the midpoint of E. The polygon representing the face has E twice on its perimeter, hence the point p appears also twice. We name them as p and p'. Which one we call p or p' does not matter. Consider a path on the perimeter of this polygon starting from p and ending up with p' according to the counter-clock wise orientation. Let r' be the total number of dots clustered around vertices of the face, counted along the path. Then it satisfies

$$0 < r' < r. \tag{2.7}$$

For example, not all r dots of a face can be clustered at a vertex of degree 1. In particular, for the case of $r = 1$, the graph γ has no edges bounding the same face twice.

An **arrowed** r-Hurwitz graph $(\gamma, \vec{D})$ has, in addition to the above data (γ, D), an arrow assigned to one of the μ_i dots from Vertex i for each index $1 \leq i \leq n$.

The counting problem we wish to study is the number $\mathcal{H}^r_{g,n}(\mu_1 \dots, \mu_n)$ of arrowed r-Hurwitz graphs for a prescribed ordered partition (2.6), counted with the automorphism weight. The combinatorial data corresponds to an object in algebraic geometry. Let us first identify what the r-Hurwitz graphs represent. We denote by $\mathbb{P}^1[r]$ the 1-dimensional orbifold modeled on $\mathbb{P}^1$ that has one stacky point $\left[0/\big(\mathbb{Z}/(r)\big)\right]$ at $0 \in \mathbb{P}^1$.

Example 2.9. The base case is $\mathcal{H}^r_{0,1}(r) = 1$ (see Figure 2.3). This counts the identity morphism $\mathbb{P}^1[r] \xrightarrow{\sim} \mathbb{P}^1[r]$.

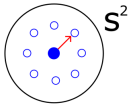

Figure 2.3 – The graph has only one vertex and no edges. All r dots are clustered around this unique vertex, with an arrow attached to one of them. Because of the arrow, there is no automorphism of this graph.

Definition 2.10 (Orbifold Hurwitz cover and Orbifold Hurwitz numbers). An *orbifold Hurwitz cover* $f : C \longrightarrow \mathbb{P}^1[r]$ is a morphism from an orbifold C that is modeled on a smooth algebraic curve of genus g that has

1. m stacky points of the same type as the one on the base curve that are all mapped to $\big[0/\big(\mathbb{Z}/(r)\big)\big] \in \mathbb{P}^1[r]$,

2. arbitrary profile $(\mu_1, \ldots, \mu_n)$ with n labeled points over $\infty \in \mathbb{P}^1[r]$,

3. and all other ramification points are simple.

If we replace the target orbifold by $\mathbb{P}^1$, then the morphism is a regular map from a smooth curve of genus g with profile $(\overbrace{r, \ldots, r}^{m})$ over $0 \in \mathbb{P}^1$, labeled profile $(\mu_1, \ldots, \mu_n)$ over $\infty \in \mathbb{P}^1$, and a simple ramification at any other ramification point. The Euler characteristic condition (2.5) of the graph γ gives the number of simple ramification points of f through the Riemann-Hurwitz formula. The automorphism weighted count of the number of the topological types of such covers is denoted by $H^r_{g,n}(\mu_1, \ldots, \mu_n)$. These numbers are referred to as *orbifold Hurwitz numbers*. When $r = 1$, they count the usual simple Hurwitz numbers.

The counting of the topological types is the same as counting actual orbifold Hurwitz covers such that all simple ramification points are mapped to one of the s-th roots of unity $\xi^1, \ldots, \xi^s$, where $\xi = \exp(2\pi i/s)$, if all simple ramification points of f are labeled. Indeed, such a labeling is given by elements of the cyclic group $\{\xi^1, \ldots, \xi^s\}$ of order s. Let us construct an edge-labeled Hurwitz graph from an orbifold Hurwitz cover with fixed branch points on the target as above. We first review the case of $r = 1$, i.e., the simple Hurwitz covers. Our graph is essentially the same as the dual of the *branching graph* of [22].

2.3. **Construction of r-Hurwitz graphs**

First we consider the case $r = 1$. Let $f : C \longrightarrow \mathbb{P}^1$ be a simple Hurwitz cover of genus g and degree d with labeled profile $(\mu_i, \ldots, \mu_n)$ over ∞,

unramified over $0 \in \mathbb{P}^1$, and simply ramified over $B = \{\xi^1, \dots, \xi^s\} \subset \mathbb{P}^1$, where $\xi = \exp(2\pi i/s)$ and $s = 2g - 2 + d + n$. We denote by $R = \{p_1, \dots, p_s\} \subset C$ the labeled simple ramification points of f, that is bijectively mapped to B by $f : R \longrightarrow B$. We choose a labeling of R so that $f(p_\alpha) = \xi^\alpha$ for every $\alpha = 1, \dots, s$.

On $\mathbb{P}^1$, plot B and connect each element $\xi^\alpha \in B$ with 0 by a straight line segment. We also connect 0 and ∞ by a straight line $z = t\exp(\pi i/s)$, $0 \le t \le \infty$. Let $*$ denote the configuration of the s line segments. The inverse image $f^{-1}(*)$ is a cell graph on C, for which $f^{-1}(0)$ forms the set of vertices. We remove all inverse images $f^{-1}(\overline{0\xi^\alpha})$ of the line segment $\overline{0\xi^\alpha}$ from this graph, except for the ones that end at one of the points $p_\alpha \in R$. Since p_α is a simple ramification point of f, the line segment ending at p_α extends to another vertex, i.e., another point in $f^{-1}(0)$. We denote by $\gamma^\vee$ the graph after this removal of line segments. We define the edges of the graph to be the connected line segments at p_α for some α. We use p_α as the label of the edge. The graph $\gamma^\vee$ has d vertices, s edges, and n faces.

An inverse image of the line $\overline{0\infty}$ is a ray starting at a vertex of the graph $\gamma^\vee$ and ending up with one of the points in $f^{-1}(\infty)$, which is the center of a face. We place a dot on this line near at each vertex. The edges of $\gamma^\vee$ incident to a vertex are cyclically ordered counter-clockwise, following the natural cyclic order of B. Let p_α be an edge incident to a vertex, and p_β the next one at the same vertex according to the cyclic order. We denote by $d_{\alpha\beta}$ the number of dots in the span of two edges p_α and p_β, which is 0 if $\alpha < \beta$, and 1 if $\beta < \alpha$. Now we consider the dual graph γ of $\gamma^\vee$. It has n vertices, d faces, and s edges still labeled by $\{p_1, \dots, p_s\}$. At the angled corner between the two adjacent edges labeled by p_α and p_β in this order according to the cyclic order, we place $d_{\alpha\beta}$ dots. The data (γ, D) consisting of the cell graph γ and the dot configuration D is the Hurwitz graph corresponding to the simple Hurwitz cover $f : C \longrightarrow \mathbb{P}^1$ for $r = 1$.

It is obvious that what we obtain is an $r = 1$ Hurwitz graph, except for the condition (5) of the configuration D, which requires an explanation. The dual graph $\gamma^\vee$ for $r = 1$ is the *branching graph* of [22]. Since $|B| = s$ is the number of simple ramification points, which is also the number of edges of $\gamma^\vee$, the branching graph cannot have any loops. This is because two distinct powers of ξ in the range of $1, \dots, s$ cannot be the same. This fact reflects in the condition that γ has no edge that bounds the same face twice. This explains the condition (5) for $r = 1$.

Remark 2.11. If we consider the case $r = 1, g = 0$ and $n = 1$, then $s = d - 1$. Hence the graph $\gamma^\vee$ is a connected tree consisting of d nodes (vertices) and $d-1$ *labeled* edges. Except for $d = 1, 2$, every vertex is uniquely

labeled by incident edges. The tree counting of Introduction is relevant to Hurwitz numbers in this way.

Now let us consider an orbifold Hurwitz cover $f : C \longrightarrow \mathbb{P}^1[r]$ of genus g and degree $d = rm$ with labeled profile $(\mu_i, \ldots, \mu_n)$ over ∞, m isomorphic stacky points over $\big[0/\big(\mathbb{Z}/(r)\big)\big] \in \mathbb{P}^1[r]$, and simply ramified over $B = \{\xi^1, \ldots, \xi^s\} \subset \mathbb{P}^1[r]$, where $s = 2g - 2 + m + n$. By $R = \{p_1, \ldots, p_s\} \subset C$ we indicate the labeled simple ramification points of f, that is again bijectively mapped to B by $f : R \longrightarrow B$. We choose the same labeling of R so that $f(p_\alpha) = \xi^\alpha$ for every $\alpha = 1, \ldots, s$.

On $\mathbb{P}^1[r]$, plot B and connect each element $\xi^\alpha \in B$ with the stacky point at 0 by a straight line segment. We also connect 0 and ∞ by a straight line $z = t\exp(\pi i/s)$, $0 \le t \le \infty$, as before. Let $*$ denote the configuration of the s line segments. The inverse image $f^{-1}(*)$ is a cell graph on C, for which $f^{-1}(0)$ forms the set of vertices. We remove all inverse images $f^{-1}(\overline{0\xi^\alpha})$ of the line segment $\overline{0\xi^\alpha}$ from this graph, except for the ones that end at one of the points $p_\alpha \in R$. We denote by $\gamma^\vee$ the graph after this removal of line segments. We define the edges of the graph to be the connected line segments at p_α for some α. We use p_α as the label of the edge. The graph $\gamma^\vee$ has m vertices, s edges.

The inverse image of the line $\overline{0\infty}$ forms a set of r rays at each vertex of the graph $\gamma^\vee$, connecting m vertices and n centers $f^{-1}(\infty)$ of faces. We place a dot on each line near at each vertex. These dots are cyclically ordered according to the orientation of C, which we choose to be counter-clock wise. The edges of $\gamma^\vee$ incident to a vertex are also cyclically ordered in the same way. Let p_α be an edge incident to this vertex, and p_β the next one according to the cyclic order. We denote by $d_{\alpha\beta}$ the number of dots in the span of two edges p_α and p_β. Let γ denote the dual graph of $\gamma^\vee$. It now has n vertices, m faces, and s edges still labeled by $\{p_1, \ldots, p_s\}$. At the angled corner between the two adjacent edges labeled by p_α and p_β in this order according to the cyclic order, we place $d_{\alpha\beta}$ dots, again cyclically ordered as on $\gamma^\vee$. The data (γ, D) consisting of the cell graph γ and the dot configuration D is the r-Hurwitz graph corresponding to the orbifold Hurwitz cover $f : C \longrightarrow \mathbb{P}^1[r]$.

We note that $\gamma^\vee$ can have loops, unlike the case of $r = 1$. Let us place $\gamma^\vee$ locally on an oriented plane around a vertex. The plane is locally separated into r sectors by the r rays $f^{-1}(\overline{0\infty})$ at this vertex. There are s half-edges coming out of the vertex at each of these r sectors. A half-edge corresponding to ξ^α cannot be connected to another half-edge corresponding to ξ^β in the same sector, by the same reason for the case of $r = 1$. But it can be connected to another half-edge of a different sector corresponding again to the same ξ^α. In this case, within the loop there are some dots, representing the rays of $f^{-1}(\overline{0\infty})$ in between these half-edges. The total number of dots in the loop cannot be r,

because then the half-edges being connected are in the same sector. Thus the condition (5) is satisfied.

Example 2.12. Theorem 2.15 below shows that

$$\mathcal{H}^2_{0,2}(3,1) = \frac{9}{2}.$$

This is the weighted count of the number of 2-Hurwitz graphs of type $(g,n,d) = (0,2,4)$ with an ordered partition $4 = 3+1$.

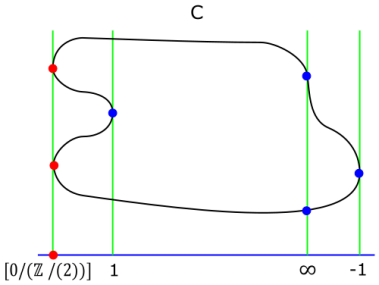

Figure 2.4 – Hurwitz covers counted in $\mathcal{H}^2_{0,2}(3,1)$ have two orbifolds points, two simple ramification points, and one ramification point of degree 3.

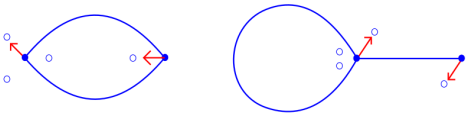

Figure 2.5 – There are two 2-Hurwitz graphs. The number of graphs is 3/2 for the graph on the left counting the automorphism, and 3 for the one on the right. The total is thus 9/2.

In terms of formulas, the 2-Hurwitz cover corresponding to the graph on the left of Figure 2.5 is given by

$$f(x) = \frac{(x-1)^2(x+1)^2}{x}.$$

To make the simple ramification points sit on ± 1, we need to divide $f(x)$ by $f(i/\sqrt{3})$, where $x = \pm 1/\sqrt{3}$ are the simple ramification points. The 2-Hurwitz cover corresponding to the graph on the right of Figure 2.5 is given by

$$f(x) = \frac{(x-1)^2(x+1)^2}{x-a},$$

where a is a real number satisfying $|a| > \sqrt{3}/2$. The real parameter a changes the topological type of the 2-Hurwitz cover. For $-\frac{\sqrt{3}}{2} < a < \frac{\sqrt{3}}{2}$, the graph is the same as on the left, and for $|a| > \frac{\sqrt{3}}{2}$, the graph becomes the one on the right.

2.4. **The edge-contraction formulas**

Definition 2.13 (Edge-contraction operations). The edge-contraction operations (ECOs) on an arrowed r-Hurwitz graph $(\gamma, \vec{D})$ are the following procedures. Choose an edge E of the cell graph γ.

• **ECO 1**. We consider the case that E is an edge connecting two distinct vertices Vertex i and Vertex j. We can assume $i < j$, which induces a direction $i \xrightarrow{E} j$ on E. Let us denote by F_+ and F_- the faces bounded by E, where F_+ is on the left side of E with respect to the direction. We now contract E, with the following additional operations:

1. Remove the original arrows at Vertices i and j.

2. Put the dots on $F_\pm$ clustered at Vertices i and j together, keeping the cyclic order of the dots on each of $F_\pm$.

3. Place a new arrow to the largest dot on the corner at Vertex i of Face F_+ with respect to the cyclic order.

4. If there are no dots on this particular corner, then place an arrow to the first dot we encounter according to the counter-clock wise rotation from E and centered at Vertex i.

The new arrow at the joined vertex allows us to recover the original graph from the new one.

• **ECO 2**. This time E is a loop incident to Vertex i twice. We contract E and separate the vertex into two new ones, as in ECO2 of Definition 2.5. The additional operations are:

1. The contraction of a loop does not change the number of faces. Separate the dots clustered at Vertex i according to the original configuration.

2. Look at the new vertex to which the original arrow is placed. We keep the same name i to this vertex. The other vertex is named i'.

3. Place a new arrow to the dot on the corner at the new Vertex i that was the largest in the original corner with respect to the cyclic order.

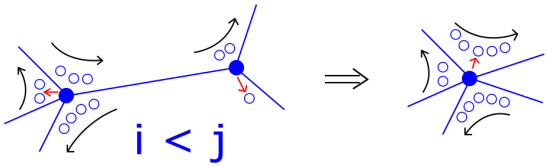

Figure 2.6 – After contracting the edge, a new arrow is placed on the dot that is the largest (according to the cyclic order) around Vertex i in the original graph, and on the face incident to E which is on the left of E with respect to the direction $i \to j$. The new arrow tells us where the break is made in the original graph. If there are no dots on this particular face, then we go around Vertex i counter-clock wise and find the first dot in the original graph. We place an arrow to this dot in the new graph after contracting E. Here again the purpose is to identify which of the μ_i dots come from the original Vertex i.

4. If there are no dots on this particular corner, then place an arrow to the first dot we encounter according to the counter-clock wise rotation from E and centered at Vertex i on the side of the old arrow.

5. We do the same operation for the new Vertex i', and put a new arrow to a dot.

6. Now remove the original arrow.

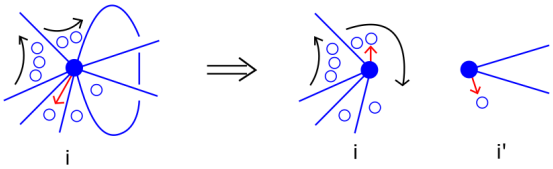

Figure 2.7 – New arrows are placed so that the original graph can be recovered from the new one.

Although cumbersome, it is easy to show that

LEMMA 2.14. *The edge-contraction operations preserve the set of r-Hurwitz graphs.*

An application of the edge-contraction operations is the following counting recursion formula.

THEOREM 2.15 (Edge-Contraction Formula). *The number of arrowed Hurwitz graphs satisfy the following edge-contraction formula.*

(2.8)

$$\begin{aligned}\left(2g-2+\frac{d}{r}+n\right)\mathcal{H}^r_{g,n}(\mu_1\ldots,\mu_n)&\\ =\sum_{i<j}\mu_i\mu_j\mathcal{H}^r_{g,n-1}(\mu_1,\ldots,\mu_{i-1},\mu_i+\mu_j,\mu_{i+1},\ldots,\widehat{\mu_j},\ldots,\mu_n)&\\ +\frac{1}{2}\sum_{i=1}^{n}\mu_i\sum_{\substack{\alpha+\beta=\mu_i\\ \alpha,\beta\geq 1}}\Bigg[\mathcal{H}^r_{g-1,n+1}(\alpha,\beta,\mu_1,\ldots,\widehat{\mu_i},\ldots,\mu_n)&\\ +\sum_{\substack{g_1+g_2=g\\ I\sqcup J=\{1,\ldots,\hat{i},\ldots,n\}}}\mathcal{H}^r_{g_1,|I|+1}(\alpha,\mu_I)\mathcal{H}^r_{g_2,|J|+1}(\beta,\mu_J)\Bigg].&\end{aligned}$$

Here, $\widehat{\ }$ indicates the omission of the index, and $\mu_I=(\mu_i)_{i\in I}$ for any subset $I\subset\{1,2,\ldots,n\}$.

Remark 2.16. The edge-contraction formula (ECF) is a recursion with respect to the number of edges

$$s=2g-2+\frac{\mu_1+\cdots+\mu_n}{r}+n.$$

Therefore, it calculates all values of $\mathcal{H}^r_{g,n}(\mu_1\ldots,\mu_n)$ from the base case $\mathcal{H}^r_{0,1}(r)$. However, it does not determine the initial value itself, since $s=0$. We also note that the recursion is not for $\mathcal{H}^r_{g,n}$ as a function in n integer variables.

Proof. The counting is done by applying the edge-contraction operations. The left-hand side of (2.8) shows the choice of an edge, say E, out of $s=2g-2+\frac{d}{r}+n$ edges. The first line of the right-hand side corresponds to the case that the chosen edge E connects Vertex i and Vertex j. We assume $i<j$, and apply ECO 1. The factor $\mu_i\mu_j$ indicates the removal of two arrows at these vertices (Figure 2.6).

When the edge E we have chosen is a loop incident to Vertex i twice, then we apply ECO 2. The factor μ_i is the removal of the original arrow (Figure 2.7). The second and third lines on the right-hand side correspond whether E is a handle-cutting loop, or a separation loop. The factor $\frac{1}{2}$ is there because of the symmetry between α and β of the partition of μ_i. This complete the proof. □

THEOREM 2.17 (Graph enumeration and orbifold Hurwitz numbers). *The graph enumeration and counting orbifold Hurwitz number are related by the following formula:*

$$\mathcal{H}^r_{g,n}(\mu_i,\dots,\mu_n) = \mu_1\mu_2\cdots\mu_n H^r_{g,n}(\mu_i,\dots,\mu_n). \tag{2.9}$$

Proof. The simplest orbifold Hurwitz number is $H^r_{0,1}(r)$, which counts double Hurwitz numbers with the same profile (r) at both $0 \in \mathbb{P}^1$ and $\infty \in \mathbb{P}^1$. There is only one such map $f : \mathbb{P}^1 \longrightarrow \mathbb{P}^1$, which is given by $f(x) = x^r$. Since the map has automorphism $\mathbb{Z}/(r)$, we have $H^r_{0,1}(r) = 1/r$. Thus (2.9) holds for the base case.

We notice that (2.8) is exactly the same as the cut-and-join equation of [1, Theorem 2.2], after modifying the orbifold Hurwitz numbers by multiplying $\mu_1\cdots\mu_n$. Since the initial value is the same, and the formulas are recursion based on $s = 2g-2+\frac{d}{r}+n$, (2.9) holds by induction. This completes the proof. □

3. CONSTRUCTION OF THE MIRROR SPECTRAL CURVES FOR ORBIFOLD HURWITZ NUMBERS

In the earlier work on simple and orbifold Hurwitz numbers in connection to the topological recursion [1, 3, 5, 13, 21], the spectral curves are determined by the infinite framing limit of the mirror curves to toric Calabi-Yau (orbi-)threefolds. The other ingredients of the topological recursion, the differential forms $W_{0,1}$ and $W_{0,2}$, are calculated by the Laplace transform of the $(g,n) = (0,1)$ and $(0,2)$ cases of the ELSV [12] and JPT [17] formulas. Certainly the logic is clear, but why these choices are the right ones is not well explained.

In this section, we show that the edge-contraction operations themselves determine all the mirror ingredients, i.e., the spectral curve, $W_{0,1}$, and $W_{0,2}$. The structure of the story is the following. The edge-contraction formula (2.8) is an equation among different values of (g,n). When restricted to $(g,n) = (0,1)$, it produces an equation on $\mathcal{H}^r_{0,1}(d)$ as a function in one integer variable. The generating function of $\mathcal{H}^r_{g,n}(\mu_1,\dots,\mu_n)$ is reasonably complicated, but it can be expressed rather nicely in terms of the generating function of the $(0,1)$-values $\mathcal{H}^r_{0,1}(d)$, which is essentially the spectral curve of the theory. The edge-contraction formula (2.8) itself has the Laplace transform that can be calculated in the spectral curve coordinate. Since (2.8) contains (g,n) on each side of the equation, to make it a genuine recursion formula for functions with respect to $2g-2+n$ in the stable range, we need to calculate the generating

functions of $\mathcal{H}^r_{0,1}(d)$ and $\mathcal{H}^r_{0,2}(\mu_1,\mu_2)$, and make the rest of (2.8) free of unstable terms. The result is the topological recursion of [1, 13].

Let us now start with the restricted (2.8) on $(0,1)$ invariants:

$$\left(\frac{d}{r}-1\right)\mathcal{H}^r_{0,1}(d)=\frac{1}{2}d\sum_{\substack{\alpha+\beta=d\\ \alpha,\beta\geq 1}}\mathcal{H}^r_{0,1}(\alpha)\mathcal{H}^r_{0,1}(\beta). \tag{3.1}$$

At this stage, we introduce a generating function

$$y=y(x)=\sum_{d=1}^{\infty}\mathcal{H}^r_{0,1}(d)x^d. \tag{3.2}$$

In terms of this generating function, (3.1) is a differential equation

$$\left(x^{r+1}\circ\frac{d}{dx}\circ\frac{1}{x^r}\right)y=\frac{1}{2}rx\frac{\mathrm{d}}{\mathrm{d}x}y^2, \tag{3.3}$$

or simply

$$\frac{y'}{y}-ry'=\frac{r}{x}.$$

Its unique solution is

$$Cx^r=ye^{-ry}$$

with a constant of integration C. As we noted in the previous section, the recursion (2.8) does not determine the initial value $\mathcal{H}^r_{0,1}(d)$. For our graph enumeration problem, the values are

$$\mathcal{H}^r_{0,1}(d)=\begin{cases}0 & 1\leq d<r;\\ 1 & d=r,\end{cases} \tag{3.4}$$

which determine $C=1$. Thus we find

$$x^r=ye^{-ry}, \tag{3.5}$$

which is the r-Lambert curve of [1]. This is indeed the spectral curve for the orbifold Hurwitz numbers.

Remark 3.1. We note that $r\mathcal{H}^r_{0,1}(rm)$ satisfies the same recursion equation (3.1) for $r=1$, with a different initial value. Thus essentially orbifold Hurwitz numbers are determined by the usual simple Hurwitz numbers.

Remark 3.2. If we define $T_d=(d-1)!\mathcal{H}^{r=1}_{0,1}(d)$, then (3.1) for $r=1$ is equivalent to (1.2). This is the reason we consider the tree recursion as the spectral curve for simple and orbifold Hurwitz numbers.

For the purpose of performing analysis on the spectral curve (3.5), let us introduce a global coordinate z on the r-Lambert curve, which is an analytic curve of genus 0:

$$\begin{cases}x=x(z):=ze^{-z^r}\\ y=y(z):=z^r.\end{cases} \tag{3.6}$$

We denote by $\Sigma \subset \mathbb{C}^2$ this parametric curve. Let us introduce the generating functions of general $\mathcal{H}^r_{g,n}$, which are called *free energies*:

$$F_{g,n}(x_1,\dots,x_n) := \sum_{\mu_1,\dots,\mu_n \geq 1} \frac{1}{\mu_1 \cdots \mu_n} \mathcal{H}^r_{g,n}(\mu_1,\dots,\mu_n) \prod_{i=1}^{n} x_i^{\mu_i}. \tag{3.7}$$

We also define the exterior derivative

$$W_{g,n}(x_1,\dots,x_n) := d_1 \cdots d_n F_{g,n}(x_1,\dots,x_n), \tag{3.8}$$

which is a symmetric n-linear differential form. By definition, we have

$$y = y(x) = x\frac{\mathrm{d}}{\mathrm{d}x} F_{0,1}(x). \tag{3.9}$$

The topological recursion requires the spectral curve, $W_{0,1}$, and $W_{0,2}$. From (3.8) and (3.9), we have

$$W_{0,1}(x) = y\frac{\mathrm{d}x}{x} = y\mathrm{d}\log(x). \tag{3.10}$$

Remark 3.3. For many examples of topological recursion such as ones considered in [11], we often define $W_{0,1} = y\mathrm{d}x$, which is a holomorphic 1-form on the spectral curve. For Hurwitz theory, due to (3.9), it is more natural to use (3.10).

As a differential equation, we can solve (3.9) in a closed formula on the spectral curve Σ of (3.6). Indeed, the role of the spectral curve is that the free energies, i.e., $F_{g,n}$'s, are actually analytic functions defined on Σ^n. Although we define $F_{g,n}$'s as a formal power series in $(x_1,\dots,x_n)$ as generating functions, they are analytic, and the domain of analyticity, or the classical sense of *Riemann surface*, is the spectral curve Σ. The coordinate change (3.6) gives us

$$x\frac{\mathrm{d}}{\mathrm{d}x} = \frac{z}{1-rz^r}\frac{\mathrm{d}}{\mathrm{d}z}, \tag{3.11}$$

hence (3.9) is equivalent to

$$z^{r-1}(1-rz^r) = \frac{\mathrm{d}}{\mathrm{d}z} F_{0,1}\big(x(z)\big).$$

Since $z = 0 \Longrightarrow x = 0 \Longrightarrow F_{0,1}(x) = 0$, we find

$$F_{0,1}\big(x(z)\big) = \frac{1}{r}z^r - \frac{1}{2}z^{2r}. \tag{3.12}$$

The calculation of $F_{0,2}$ is done similarly, by restricting (2.8) to the $(g,n) = (0,1)$ and $(0,2)$ terms. Assuming that $\mu_1 + \mu_n = mr$, we have

$$\left(\frac{d}{r} - 1\right) \mathcal{H}^r_{0,2}(\mu_1,\mu_2) \tag{3.13}$$

$$= \mu_1\mu_2\mathcal{H}^r_{0,1}(\mu_1+\mu_2) + \mu_1 \sum_{\substack{\alpha+\beta=\mu_1\\ \alpha,\beta>0}} \mathcal{H}^r_{0,1}(\alpha)\mathcal{H}^r_{0,2}(\beta,\mu_2) + \mu_2 \sum_{\substack{\alpha+\beta=\mu_2\\ \alpha,\beta>0}} \mathcal{H}^r_{0,1}(\alpha)\mathcal{H}^r_{0,2}(\mu_1,\beta).$$

As a special case of [1, Lemma 4.1], this equation translates into a differential equation for $F_{0,2}$:

$$\begin{aligned}
&\frac{1}{r}\left(x_1\frac{\partial}{\partial x_1}+x_2\frac{\partial}{\partial x_2}\right)F_{0,2}(x_1,x_2)\\
&\quad=\frac{1}{x_1-x_2}\left(x_1^2\frac{\partial}{\partial x_1}F_{0,1}(x_1)-x_2^2\frac{\partial}{\partial x_2}F_{0,1}(x_2)\right)\\
&\quad\quad-\left(x_1\frac{\partial}{\partial x_1}F_{0,1}(x_1)+x_2\frac{\partial}{\partial x_2}F_{0,1}(x_2)\right)\\
&\quad\quad+\left(x_1\frac{\partial}{\partial x_1}F_{0,1}(x_1)\right)\left(x_1\frac{\partial}{\partial x_1}F_{0,2}(x_1,x_2)\right)\\
&\quad\quad+\left(x_2\frac{\partial}{\partial x_2}F_{0,1}(x_2)\right)\left(x_2\frac{\partial}{\partial x_2}F_{0,2}(x_1,x_2)\right).
\end{aligned} \tag{3.14}$$

Denoting by $x_i = x(z_i)$ and using (3.11), (3.14) becomes simply

$$\frac{1}{r}\left(z_1\frac{\partial}{\partial z_1}+z_2\frac{\partial}{\partial z_2}\right)F_{0,2}\big(x(z_1),x(z_2)\big)=\frac{x_1z_1^r-x_2z_2^r}{x_1-x_2}-(z_1^r+z_2^r) \tag{3.15}$$

on the spectral curve Σ. This is a linear partial differential equation of the first order with analytic coefficients in the neighborhood of $(0,0)\in\mathbb{C}^2$, hence by the Cauchy-Kovalevskaya theorem, it has the unique analytic solution around the origin of $\mathbb{C}^2$ for any Cauchy problem. Since the only analytic solution to the homogeneous equation

$$\left(z_1\frac{\partial}{\partial z_1}+z_2\frac{\partial}{\partial z_2}\right)f(z_1,z_2)=0$$

is a constant, the initial condition $F_{0,2}(0,x_2)=F_{0,2}(x_1,0)=0$ determines the unique solution of (3.15).

Proposition 3.4. *We have a closed formula for $F_{0,2}$ in the z-coordinates:*

$$F_{0,2}\big(x(z_1),x(z_2)\big)=\log\frac{z_1-z_2}{x(z_1)-x(z_2)}-(z_1^r+z_2^r). \tag{3.16}$$

Proof. We first note that $\log\frac{z_1-z_2}{x(z_1)-x(z_2)}$ is holomorphic around $(0,0)\in\mathbb{C}^2$. (3.16) being a solution to (3.15) is a straightforward calculation that can be

verified as follows:

$$\begin{aligned}&\left(z_1\frac{\partial}{\partial z_1}+z_2\frac{\partial}{\partial z_2}\right)\log\frac{z_1-z_2}{x(z_1)-x(z_2)}\\&=\frac{z_1-z_2}{z_1-z_2}-\frac{z_1e^{-z_1^r}(1-rz_1^r)-z_2e^{-z_2^r}(1-rz_2^r)}{x_1-x_2}\\&=1-\frac{x_1-x_2}{x_1-x_2}+r\frac{x_1z_1^r-x_2z_2^r}{x_1-x_2}=r\frac{x_1z_1^r-x_2z_2^r}{x_1-x_2}.\end{aligned}$$

Since $F_{0,2}\big(x(0),x(z_2)\big)=\log e^{z_2^r}-z_2^r=0$, (3.16) is the desired unique solution. □

In [1], the functions (3.12) and (3.16) are derived by directly computing the Laplace transform of the JPT formulas [17]

(3.17)

$$H^r_{0,1}(d)=\frac{d^{\lfloor\frac{d}{r}\rfloor-2}}{\lfloor\frac{d}{r}\rfloor!},$$

$$H^r_{0,2}(\mu_1,\mu_2)=\begin{cases}r^{\langle\frac{\mu_1}{r}\rangle+\langle\frac{\mu_1}{r}\rangle}\frac{1}{\mu_1+\mu_2}\frac{\mu_1^{\lfloor\frac{\mu_1}{r}\rfloor}\mu_2^{\lfloor\frac{\mu_2}{r}\rfloor}}{\lfloor\frac{\mu_1}{r}\rfloor!\lfloor\frac{\mu_2}{r}\rfloor!} & \mu_1+\mu_2\equiv 0 \mod r\\ 0 & \text{otherwise.}\end{cases}$$

Here, $q=\lfloor q\rfloor+\langle q\rangle$ gives the decomposition of a rational number $q\in\mathbb{Q}$ into its floor and the fractional part. We have thus recovered (3.17) from the edge-contraction formula alone, which are the $(0,1)$ and $(0,2)$ cases of the ELSV formula for the orbifold Hurwitz numbers.

Acknowledgments. The paper is based a series of lectures by M.M. at Mathematische Arbeitstagung 2015, Max-Planck-Institut für Mathematik in Bonn. The authors are grateful to the American Institute of Mathematics in California, the Banff International Research Station, the Institute for Mathematical Sciences at the National University of Singapore, Kobe University, Leibniz Universität Hannover, the Lorentz Center for Mathematical Sciences, Leiden, Max-Planck-Institut für Mathematik in Bonn, and Institut Henri Poincaré, Paris, for their hospitality and financial support during the authors' stay for collaboration. The research of O.D. has been supported by GRK 1463 *Analysis, Geometry, and String Theory* at Leibniz Universität Hannover and MPIM. The research of M.M. has been supported by NSF grants DMS-1309298, DMS-1619760, DMS-1642515, and NSF-RNMS: Geometric Structures And Representation Varieties (GEAR Network, DMS-1107452, 1107263, 1107367).

REFERENCES

[1] V. Bouchard, D. Hernández Serrano, X. Liu, and M. Mulase, *Mirror symmetry for orbifold Hurwitz numbers*. Preprint arXiv:1301.4871 [math.AG], 2013.

[2] V. Bouchard, A. Klemm, M. Mariño, and S. Pasquetti, *Remodeling the B-model*. Commun. Math. Phys. **287** (2009), 117–178.

[3] V. Bouchard and M. Mariño, *Hurwitz numbers, matrix models and enumerative geometry*. Proc. Symposia Pure Math. **78** (2008), 263–283.

[4] R. Dijkgraaf, E. Verlinde, and H. Verlinde, *Loop equations and Virasoro constraints in non-perturbative two-dimensional quantum gravity*. Nucl. Phys. **B348** (1991), 435–456.

[5] N. Do, O. Leigh, and P. Norbury, *Orbifold Hurwitz numbers and Eynard-Orantin invariants*. Preprint arXiv:1212.6850, 2012.

[6] O. Dumitrescu and M. Mulase, *Quantum curves for Hitchin fibrations and the Eynard-Orantin theory*. Lett. Math. Phys. **104** (2014), 635–671.

[7] O. Dumitrescu and M. Mulase, *Quantization of spectral curves for meromorphic Higgs bundles through topological recursion*. Preprint arXiv:1411.1023, 2014.

[8] O. Dumitrescu and M. Mulase, *Edge contraction on dual ribbon graphs and 2D TQFT*. Journal of Algebra **494** (2018), 1–27.

[9] O. Dumitrescu and M. Mulase, *Lectures on the topological recursion for Higgs bundles and quantum curves*. To appear in the Lecture Notes Series of the National University of Singapore.

[10] O. Dumitrescu and M. Mulase, *An invitation to 2D TQFT and quantization of Hitchin spectral curves*. Banach Center Publications **114** (2018), 85–144.

[11] O. Dumitrescu, M. Mulase, A. Sorkin and B. Safnuk, *The spectral curve of the Eynard-Orantin recursion via the Laplace transform*. In: Dzhamay, Maruno and Pierce (eds.), *Algebraic and Geometric Aspects of Integrable Systems and Random Matrices*, Contemporary Mathematics **593** (2013), pp. 263–315.

[12] T. Ekedahl, S. Lando, M. Shapiro, and A. Vainshtein, *Hurwitz numbers and intersections on moduli spaces of curves*. Invent. Math. **146** (2001), 297–327.

[13] B. Eynard, M. Mulase and B. Safnuk, *The Laplace transform of the cut-and-join equation and the Bouchard-Mariño conjecture on Hurwitz numbers*. Publications of the Research Institute for Mathematical Sciences **47** (2011), 629–670.

[14] B. Eynard and N. Orantin, *Invariants of algebraic curves and topological expansion*. Communications in Number Theory and Physics **1** (2007), 347–452.

[15] B. Fang, C.-C. M. Liu, and Z. Zong, *All genus open-closed mirror symmetry for affine toric Calabi-Yau 3-orbifolds*. Preprint arXiv:1310.4818 [math.AG], 2013.

[16] B. Fang, C.-C. M. Liu, and Z. Zong, *On the Remodeling Conjecture for Toric Calabi-Yau 3-Orbifolds*. Preprint arXiv:1604.07123, 2016.

[17] P. Johnson, R. Pandharipande, and H.H. Tseng, *Abelian Hurwitz-Hodge integrals*. Michigan Math. J. **60** (2011), 171–198.

[18] M. Kontsevich, *Intersection theory on the moduli space of curves and the matrix Airy function*. Communications in Mathematical Physics **147** (1992), 1–23.

[19] M. Mulase and M. Penkava, *Ribbon graphs, quadratic differentials on Riemann surfaces, and algebraic curves defined over* $\overline{\mathbb{Q}}$. The Asian Journal of Mathematics **2** (1998), *4*, 875–920.

[20] M. Mulase and P. Sułkowski, *Spectral curves and the Schrödinger equations for the Eynard-Orantin recursion*. Preprint arXiv:1210.3006, 2012.

[21] M. Mulase and N. Zhang, *Polynomial recursion formula for linear Hodge integrals*. Communications in Number Theory and Physics **4** (2010), 267–294.

[22] A. Okounkov and R. Pandharipande, *Gromov-Witten theory, Hurwitz numbers, and matrix models, I.* Proc. Symposia Pure Math. **80** (2009), 325–414 .

[23] C. Teleman, *The structure of 2D semi-simple field theories.* Inventiones Mathematicae **188** (2012), 525–588.

[24] G. 't Hooft, *A planer diagram theory for strong interactions.* Nuclear Physics **B 72** (1974), 461–473.

[25] E. Witten, *Two dimensional gravity and intersection theory on moduli space.* Surveys in Differential Geometry **1** (1991), 243–310.

University of North Carolina at Chapel Hill
340 Phillips Hall
CB# 3250, Chapel Hill, NC 27599-3250
dolivia@unc.edu
and
"Simion Stoilow" Institute of Mathematics
of the Romanian Academy
Calea Grivitei 21, 010702 Bucharest, Romania

University of California, Davis
Department of Mathematics
Davis, CA 95616–8633
mulase@math.ucdavis.edu
and
The University of Tokyo
Kavli Institute for Physics and
Mathematics of the Universe
Kashiwa, Japan